Proceedings of the
2005 IEEE Conference on Control Applications
Toronto, Canada, August 28-31, 2005

Motion Control of Two-Link Flexible-Joint Robot with Actuator Nonlinearities, Using Neural Networks and Direct Method

Withit Chatlatanagulchai and Peter H. Meckl, *Member, IEEE*

Abstract— **We present a state-feedback control of a two-link flexible-joint robot. We use three-layer neural networks to learn the unknown parts of the desired control laws. Therefore, the control algorithm does not require the mathematical model representing the robot. The neural networks' weights are adapted on-line. Therefore, the control system can adapt to changes during operation such as payload changes. We use a smooth variable structure controller to handle uncertainties from the neural network approximation, external disturbances, deadzone, and backlash. In our simulation, we obtain the actual plant model from experiments.**

I. Introduction

CONTROL designers should explicitly include joint flexibility in their design because joint resonant frequencies, which are located within the control bandwidth, can be excited and cause severe oscillations. The experiment in [1] suggested that the designers should consider joint flexibility in both modeling and control design.

References [2] and [3] offer two choices of slow and fast variables in order to transform the dynamical model of the flexible-joint robot into the standard singular perturbation form. Slow-control input, which adds damping to the system, drives the closed-loop system to a quasi-steady state system that has the structure of a rigid-joint robot. Then, fast-control input can be designed using available techniques for the rigid-joint robot.

Reference [4] presents a static feedback linearization method. Under the assumption that the kinetic energy of the motor is due mainly to its own rotation, the flexible-joint robot model is feedback linearizable. Reference [5] relaxes this assumption, and applies the so-called dynamic feedback linearization method to a more general robot model. Reference [6] offers a good comparison of three types of controllers: controller developed from decoupled model, backstepping controller, and passivity-based controller.

Newer results use intelligent systems to learn some or all of the unknown parts of the robot model. Reference [7] extends the work in [2] to the case where model uncertainties exist in the system. They use radial basis function networks to estimate unknown functions, and use discontinuous variable-structure controller to provide robustness to the closed-loop system. Reference [8] uses combinations of orthonormal basis functions to estimate unknown functions; they also present an experimental result of one-link flexible-joint robot. Reference [9] uses feedback linearization method and Takagi-Sugeno fuzzy system to replace model uncertainties.

This paper has the following features:

1) We consider a trajectory-tracking task of a two-link flexible-joint robot in the horizontal plane. The second motor is attached to the first link and its shaft does not share the same axis with the axis of rotation of the second link. This setting is more practical than those of shared axes commonly treated in the existing literature.

2) We obtain a model of the actual robot using the Euler-Lagrange method. This model is used as the actual robot in our simulation. We obtain parameter values of the model from real experiments with a robot in our laboratory.

3) We consider the case where deadzone and backlash exist as actuator nonlinearities. We only require their magnitude to be bounded. We do not need additional sensors to measure their magnitude. We also add external additive disturbances, commonly found in practice as measurement noise or vibration, to our Euler-Lagrange model.

4) The controller algorithm does not require a closed-form mathematical model of the robot. We design control laws from Lyapunov's second method using backstepping structure. Then, three-layer neural networks are used to estimate the unknown parts of the desired control laws – usually called direct method by adaptive control community. We use variable structure controller to provide robustness to the system against uncertainties from the estimation errors, actuator nonlinearities, and external disturbances.

5) We are able to control the trajectory of the robot effectively using link angular position, link angular velocity, motor angular position, and motor angular velocity. Existing work usually requires, in addition to the quantities above, link angular acceleration and jerk, or flexible-joint torque.

6) Due to the online adaptability of the neural networks, the controller is effective even when plant parameters change during operation. We show this by allowing payload change in our simulation.

We organize this paper as follows. Section II contains the Euler-Lagrange model of the robot, and actuator nonlinearity models. Section III contains three-layer neural network background and controller design. Section IV contains simulation results. Section V is a conclusion of the paper.

Manuscript received February 18, 2005.

The authors are with Motion and Vibration Control Laboratory, School of Mechanical Engineering, Purdue University, West Lafayette, IN 47907-2088 USA (e-mail: chatlata@purdue.edu, meckl@purdue.edu; phone: 765-494-0539; fax: 765-494-5686).

II. Robot Model

A. Dynamic Model

Consider the schematic diagram of a two-link flexible-joint robot in Fig. 1. This robot operates in the horizontal plane. Table I contains the description of parameters of the robot.

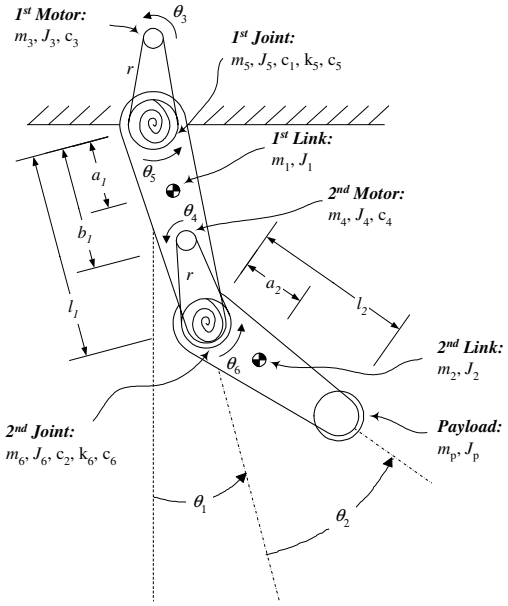

Fig. 1. Schematic diagram of a planar two-link flexible-joint robot.

TABLE I
Description of Parameters Used in the Modeling of the Two-Link Flexible-Joint Robot

1st Link	θ_1 : Absolute angular position m_1 : Lumped mass J_1 : Moment of inertia about COG a_1 : Distance between COG of the 1st link and the 1st joint b_1 : Distance between the 1st joint and the 2nd motor l_1 : Distance between the 1st joint and the 2nd joint
2nd Link	θ_2 : Relative angular position to θ_1 m_2 : Lumped mass J_2 : Moment of inertia about COG a_2 : Distance between COG of the 2nd link and the 2nd joint l_2 : Distance between the 2nd joint and the end-effector
1st Motor	θ_3 : Absolute angular position m_3 : Lumped mass J_3 : Inertia of the motor about COG c_3 : Coefficient of friction in the bearing of the motor
2nd Motor	θ_4 : Relative angular position to θ_1 m_4 : Lumped mass J_4 : Inertia of the motor about COG c_4 : Coefficient of friction in the bearing of the motor
1st Sprocket	θ_5 : Absolute angular position after gear reduction, θ_3 / r m_5 : Lumped mass J_5 : Moment of inertia about COG c_1 : Coefficient of friction in the bearing of the joint
1st Spring	k_5 : Coefficient of the torsional spring c_5 : Internal damping of the torsional spring
2nd Sprocket	θ_6 : Relative angular position after gear reduction, θ_4 / r m_6 : Lumped mass J_6 : Moment of inertia about COG c_2 : Coefficient of friction in the bearing of the joint
2nd Spring	k_6 : Coefficient of the torsional spring c_6 : Internal damping of the torsional spring
Payload	m_p : Lumped mass J_p : Moment of inertia about COG
Chain	r : Gear ratio

$x_1 = [\theta_1, \theta_2]^T$ and $x_2 = [\dot{\theta}_1, \dot{\theta}_2]^T$ represent link position and velocity, $x_3 = [\theta_5, \theta_6]^T$ and $x_4 = [\dot{\theta}_5, \dot{\theta}_6]^T$ represent sprocket position and velocity, and $T = [T_1, T_2]^T$ represent input torque.

Let $d_{ai}(\bar{x}_4) = [d_{ai1}, d_{ai2}]^T$ be bounded disturbances that may depend on all states. We, then, obtain the following state-space model

$$\begin{aligned} \dot{x}_1 &= x_2 + d_{a1}(\bar{x}_4), \\ \dot{x}_2 &= f_2(\bar{x}_2) + g_2(\bar{x}_2)\left(x_3 + d_{a2}(\bar{x}_4)\right), \\ \dot{x}_3 &= x_4 + d_{a3}(\bar{x}_4), \\ \dot{x}_4 &= f_4(\bar{x}_4) + g_4(\bar{x}_4)\left(T + d_{a4}(\bar{x}_4)\right), \\ y &= x_1, \end{aligned} \tag{1}$$

where

$$f_2 = -M^{-1}\left[Vx_2 + F_1 + K_1(x_1)\right] = [f_{21}, f_{22}]^T,$$

$$g_2 = M^{-1}K_1 = \begin{bmatrix} g_{211} & g_{212} \\ g_{221} & g_{222} \end{bmatrix}, \; g_4 = J^{-1} = \begin{bmatrix} g_{411} & g_{412} \\ g_{421} & g_{422} \end{bmatrix},$$

$$f_4 = -J^{-1}\left[F_2 - K_2(x_1 - x_3)\right] = [f_{41}, f_{42}]^T.$$

M is inertia matrix. V represents coriolis and centrifugal functions. K_1, K_2 are joint flexibility matrices. F_1, F_2 are viscous friction vectors. J represents inertia of motors and sprockets.

To closely simulate the actual robot, we obtain the parameter values from actual experiments as follows:

$$M(x_1) = \begin{bmatrix} 0.201 + 0.06\cos\theta_2 & 0.0266 + 0.03\cos\theta_2 \\ 0.0266 + 0.03\cos\theta_2 & 0.0266 \end{bmatrix},$$

$$J = \begin{bmatrix} 0.017 & 0 \\ 0 & 0.014 \end{bmatrix}, \; K_1 = \begin{bmatrix} 0.4 & 0 \\ 0 & 0.4 \end{bmatrix}, \; K_2 = \begin{bmatrix} 0.075 & 0 \\ 0 & 0.075 \end{bmatrix},$$

$$V(x_1, x_2) = \begin{bmatrix} 0 & -0.03(2\dot{\theta}_1 + \dot{\theta}_2)\sin\theta_2 \\ 0.03\dot{\theta}_1 \sin\theta_2 & 0 \end{bmatrix},$$

$$F_1(x_2) = \begin{bmatrix} 0.02\dot{\theta}_1 & 0.02\dot{\theta}_2 \end{bmatrix}^T, \; F_2(x_4) = \begin{bmatrix} 0.056\dot{\theta}_5 & 0.056\dot{\theta}_6 \end{bmatrix}^T.$$

We will use this plant to represent the actual robot in our simulation in Section IV.

B. Actuator Nonlinearities

A mathematical model of the deadzone is given in [10] as

$$\tau = \begin{cases} m^-(u - d^-), & u \le d^-, \\ 0, & d^- < u < d^+, \\ m^+(u - d^+), & u \ge d^+, \end{cases} \tag{2}$$

where τ is output of the deadzone model, u is input to the model, m^-, m^+, d^+ are positive numbers, and d^- is a

negative number.

A backlash model as in [11] is given by

$$\dot{T} = \begin{cases} m\dot{\tau}, & \text{if } \dot{\tau} > 0 \text{ and } T = m(\tau - d^+) \text{ or} \\ & \text{if } \dot{\tau} < 0 \text{ and } T = m(\tau - d^-), \\ 0, & \text{otherwise}, \end{cases} \tag{3}$$

where T is output of backlash model, τ is input to the model, m, d^+ are positive numbers and d^- is a negative number.

Fig. 2 depicts the overall plant model where u is the designed control input, τ is output of the deadzone model and T is output of the backlash model which is the input torque that actually drives the manipulator.

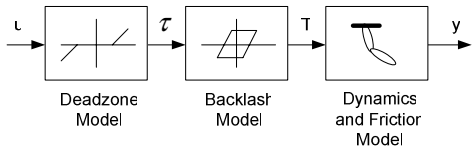

Fig. 2. Deadzone and backlash models are incorporated into the dynamical model of the two-link flexible-joint manipulators.

III. Controller Design

First, we discuss basics of the three-layer neural network. Then, we discuss controller design.

A. Three-Layer Neural Network

Fig. 3 depicts a three-layer neural network. The variables in the network are defined as follows:

$$\bar{Z} = [z_1, z_2, \ldots, z_n, 1]^T \in \mathbb{R}^{n+1},$$

$$V = [v_1, v_2, \ldots, v_l] \in \mathbb{R}^{(n+1)\times l},$$

$$v_i = [v_{i1}, v_{i2}, \ldots, v_{i(n+1)}]^T \in \mathbb{R}^{n+1}, i = 1, 2, \ldots, l,$$

$$S(V^T\bar{Z}) = [s(v_1^T\bar{Z}), s(v_2^T\bar{Z}), \ldots, s(v_l^T\bar{Z}), 1]^T \in \mathbb{R}^{l+1},$$

$$W = [w_1, w_2, \ldots, w_l, w_{l+1}]^T \in \mathbb{R}^{l+1},$$

$$h(W, V, z_1, z_2, \ldots, z_n) = W^T S(V^T\bar{Z}) \in \mathbb{R}.$$

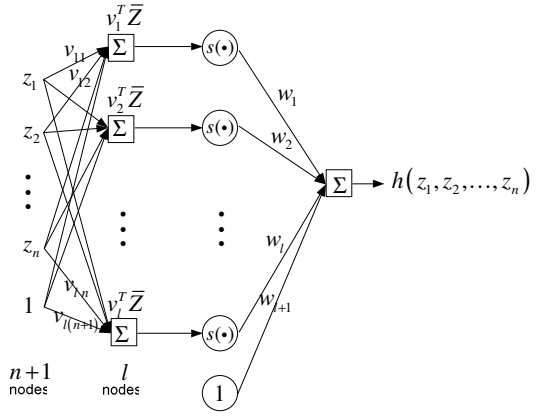

Fig. 3. A three-layer neural network. The square represents node whose output contains adjustable parameters.

$s(\bullet)$ is a sigmoid function

$$s(x) = 1/(1 + e^{-x}), \forall x \in \mathbb{R}.$$

From the universal approximation property, as was proved in [12], we have

$$h(z_1, z_2, \ldots, z_n) = W^{*T} S(V^{*T}\bar{Z}) + \varepsilon, \tag{4}$$

where $\|\varepsilon\| < \varepsilon_U$ is approximation error with unknown $\varepsilon_U > 0$ provided that $h(\cdot)$ is defined on a compact set Ω_z.

Assumption 1: On the compact set Ω_z, the ideal neural network weights W^*, V^* are constant and bounded by $\|W^*\| \le W_U$, $\|V^*\|_F \le V_U$, $i = 1, \ldots, m$, where W_U and V_U are unknown.

Let $\hat{W}$ and $\hat{V}$ be the estimates of W^* and V^*, respectively. The estimate of the function h is given by

$$\hat{h}(z_1, z_2, \ldots, z_n) = \hat{W}^T S(\hat{V}^T\bar{Z}). \tag{5}$$

By using Lemma 3.6 in [13], the differences between neural network outputs with ideal and estimated weights are given by

$$\begin{aligned} \hat{W}^T S(\hat{V}^T\bar{Z}) - W^{*T} S(V^{*T}\bar{Z}) &= \tilde{W}^T(\hat{S} - \hat{S}'\hat{V}^T\bar{Z}) \\ &\quad + \hat{W}^T\hat{S}'\tilde{V}^T\bar{Z} + d_u, \end{aligned} \tag{6}$$

where

$$\tilde{W} = \hat{W} - W^*, \tilde{V} = \hat{V} - V^*, \hat{S} = S(\hat{V}^T\bar{Z}) \in \mathbb{R}^{l+1},$$

$$\hat{S}' = diag\{\hat{s}_1', \hat{s}_2', \ldots, \hat{s}_l', 0\} \in \mathbb{R}^{(l+1)\times(l+1)},$$

$$\hat{s}_i' = s'(\hat{v}_i^T\bar{Z}) = d[s(z_a)]/dz_a\big|_{z_a = \hat{v}_i^T\bar{z}} \in \mathbb{R}, i = 1, 2, \ldots, l,$$

$$s(x) = 1/(1 + e^{-x}), \forall x \in \mathbb{R}.$$

The residual term d_u is bounded by

$$|d_u| \le \|V^*\|_F \left\|\bar{Z}\hat{W}^T\hat{S}'\right\|_F + \|W^*\|\left\|\hat{S}'\hat{V}^T\bar{Z}\right\| + |W^*|_1. \tag{7}$$

B. Backstepping and Variable Structure Controller

In this section, we design a controller that makes link angular positions θ_1 and θ_2 track desired values whereas all closed-loop signals remain bounded. We require the following assumptions.

Assumption 2: The additive disturbance $d_{aik}(\bar{x}_4)$, where $i = 1, \ldots, 4$, $k = 1, 2$, is bounded by $\|d_{aik}(\bar{x}_4)\| < d_{aikU}$, where d_{aikU} is an unknown constant.

Assumption 3: The inverses of $g_i, \forall i = 2, 4$, matrices in (1) are positive definite.

Assumption 4: The desired trajectory x_{1d} is sufficiently smooth.

Assumption 5: There exists an unknown constant $T_{iU} > 0$ such that $\|T_i - u_i\| \le T_{iU}$, $\forall i = 1, 2$.

Let $e_i = [e_{i1}, e_{i2}]^T = x_i - x_{id}$, $i = 1, \ldots, 4$ be the errors.

Step 1:

Let the virtual control law of the first subsystem be

$$x_{2d} = -c_1 e_1 + \dot{x}_{1d} + u_{2dvsc} = [x_{21d}, x_{22d}]^T,$$

where c_1 is a positive design parameter, u_{2dvsc} is variable structure control law to be designed. From Assumption 2, we have the following inequality

$$\|d_{a1j}(\bar{x}_4)\| \le K_{1j}^{*T}\phi_{1j}, \forall j = 1, 2,$$

where $K_{1j}^* = d_{a1jU}$, $\phi_{1j} = 1$.

We let the smooth variable structure control law be in the form $u_{2dvsc} = [u_{2dvsc1}, u_{2dvsc2}]^T$, where

$$u_{2dvscj} = -\hat{K}_{1j}\bar{\phi}_{1j} = -\hat{K}_{1j}\left(\frac{2}{\pi}\arctan\left(\frac{e_{1j}}{\mu_{1j}}\right)\right),$$

μ_{1j} is a small positive design parameter, $\hat{K}_{1j}$ approximates K_{1j}^* with error given by $\tilde{K}_{1j} = \hat{K}_{1j} - K_{1j}^*$.

The time derivative of the error of the first subsystem becomes

$$\begin{aligned}\dot{e}_1 &= \dot{x}_1 - \dot{x}_{1d} = (x_2 + d_{a1}) - \dot{x}_{1d} = (e_2 + x_{2d} + d_{a1}) - \dot{x}_{1d} \\ &= e_2 - c_1 e_1 + u_{2dvsc} + d_{a1}.\end{aligned}$$

Let the weight update law be

$$\dot{\hat{K}}_{1j} = \Gamma_{k1j}[\bar{\phi}_{1j} e_{1j} - \sigma_{k1j}\hat{K}_{1j}],$$

where $\Gamma_{k1j} > 0, \sigma_{k1j} > 0, \forall j = 1, 2.$

Using the following facts

$$\begin{aligned}&2\tilde{K}^T\hat{K} = \left\|\tilde{K}\right\|^2 + \left\|\hat{K}\right\|^2 - \left\|K^*\right\|^2 \geq \left\|\tilde{K}\right\|^2 - \left\|K^*\right\|^2, \\ &0 \leq |\alpha| - \alpha\frac{2}{\pi}\arctan\left(\frac{\alpha}{\mu}\right) \leq 0.2785\mu, \forall \alpha \in \mathbb{R},\end{aligned} \tag{8}$$

the time derivative of the Lyapunov function

$$V_1 = \frac{1}{2}e_1^T e_1 + \frac{1}{2}\sum_{j=1}^{2}\tilde{K}_{1j}^T\Gamma_{k1j}^{-1}\tilde{K}_{1j},$$

is given by

$$\begin{aligned}\dot{V}_1 &= e_1^T\dot{e}_1 + \sum_{j=1}^{2}\tilde{K}_{1j}^T\Gamma_{k1j}^{-1}\dot{\hat{K}}_{1j} \\ &\leq e_1^T e_2 - e_1^T c_1 e_1 - \sum_{j=1}^{2}\sigma_{k1j}\left\|\tilde{K}_{1j}\right\|^2/2 + \xi_1,\end{aligned}$$

where

$$\xi_1 = \sum_{j=1}^{2}\left(0.2785\mu_{1j}d_{a1jU} + \sigma_{k1j}\left\|K_{1j}^*\right\|^2/2\right).$$

Step 2:

The time-derivative of the error of the second subsystem is given by

$$\dot{e}_2 = \dot{x}_2 - \dot{x}_{2d} = f_2 + g_2(x_3 + d_{a2}) - \dot{x}_{2d}.$$

Suppose we know f_2 and g_2, and assume there is no disturbance d_{a1} and d_{a2} for now, then we can choose the virtual control input as

$$x_{3d}^* = -e_1 - c_2 e_2 - g_2^{-1}(f_2 - \dot{x}_{2d}). \tag{9}$$

Using the Lyapunov function $V_2 = e_1^T e_1/2 + e_2^T g_2^{-1} e_2/2$, we have $\dot{V}_2 = -c_1 e_1^T e_1 - c_2 e_2^T e_2$ which is negative definite, therefore, the errors e_1 and e_2 converge to zero.

Since we do not know f_2 and g_2, we need to modify the ideal control input x_{3d}^*. From (9), the unknown part is $h_2^*(Z_2) \triangleq g_2(\bar{x}_2)^{-1}[f_2(\bar{x}_2) - \dot{x}_{2d}] = \left[h_{21}^*, h_{22}^*\right]^T \in \mathbb{R}^2$, where h_{2j}^* is a scalar-valued continuous function of x_1, x_2, and $\dot{x}_{2jd}$. We proceed by estimating each unknown part using a three-layer neural network. From (4), we have

$$x_{3d}^* = -e_1 - c_2 e_2 - \begin{bmatrix} W_{21}^{*T} S_{21}(V_{21}^{*T}\bar{Z}_{21}) - \varepsilon_{21} \\ W_{22}^{*T} S_{22}(V_{22}^{*T}\bar{Z}_{22}) - \varepsilon_{22}\end{bmatrix}.$$

W_{2j}^* and V_{2j}^* are unknown. Let $\hat{W}_{2j}$ and $\hat{V}_{2j}$ be their estimates and add smooth variable structure control law to handle the uncertainties, we have the virtual control law

$$x_{3d} = -e_1 - c_2 e_2 - \begin{bmatrix} \hat{W}_{21}^T S_{21}(\hat{V}_{21}^T\bar{Z}_{21}) \\ \hat{W}_{22}^T S_{22}(\hat{V}_{22}^T\bar{Z}_{22})\end{bmatrix} + u_{3dvsc} = \left[x_{31d}, x_{32d}\right]^T.$$

From (4), (7), and Assumption 2, we have

$$\left|d_{u2j}\right| + \left|\varepsilon_{2j}\right| + \left|d_{a2j}\right| \leq K_{2j}^{*T}\phi_{2j},$$

where

$$\begin{aligned}K_{2j}^* &= \left[\left\|V_{2j}^*\right\|_F,\ \left\|W_{2j}^*\right\|,\ \left\|W_{2j}^*\right\|_1 + \varepsilon_{2jU} + d_{a2jU}\right]^T, \\ \phi_{2j} &= \left[\left\|\bar{Z}_{2j}\hat{W}_{2j}^T\hat{S}_{2j}^{'}\right\|_F,\ \left\|\hat{S}_{2j}^{'}\hat{V}_{2j}^T\bar{Z}_{2j}\right\|,\ 1\right]^T, \forall j = 1, 2.\end{aligned}$$

We let the smooth variable structure control law be $u_{3dvsc} = \left[u_{3dvsc1}, u_{3dvsc2}\right]^T$, where

$$u_{3dvscj} = -\hat{K}_{2j}{}^T\bar{\phi}_{2j},$$

$$\bar{\phi}_{2j} = \begin{bmatrix} \left\|\bar{Z}_{2j}\hat{W}_{2j}^T\hat{S}_{2j}^{'}\right\|_F \dfrac{2}{\pi}\arctan\left(\dfrac{e_{2j}}{\mu_{2j}}\left\|\bar{Z}_{2j}\hat{W}_{2j}^T\hat{S}_{2j}^{'}\right\|_F\right) \\ \left\|\hat{S}_{2j}^{'}\hat{V}_{2j}^T\bar{Z}_{2j}\right\|\dfrac{2}{\pi}\arctan\left(\dfrac{e_{2j}}{\mu_{2j}}\left\|\hat{S}_{2j}^{'}\hat{V}_{2j}^T\bar{Z}_{2j}\right\|\right) \\ \dfrac{2}{\pi}\arctan\left(\dfrac{e_{2j}}{\mu_{2j}}\right)\end{bmatrix}.$$

The time derivative of the error of the second subsystem becomes

$$\dot{e}_2 = g_2\left\{\begin{bmatrix} e_3 - e_1 - c_2 e_2 \\ \varepsilon_{21} - \tilde{W}_{21}{}^T(\hat{S}_{21} - \hat{S}_{21}^{'}\hat{V}_{21}{}^T\bar{Z}_{21}) \\ -\hat{W}_{21}{}^T\hat{S}_{21}^{'}\tilde{V}_{21}{}^T\bar{Z}_{21} - d_{u21} - \hat{K}_{21}{}^T\bar{\varphi}_{21} + d_{a21} \\ \varepsilon_{22} - \tilde{W}_{22}{}^T(\hat{S}_{22} - \hat{S}_{22}^{'}\hat{V}_{22}{}^T\bar{Z}_{22}) \\ -\hat{W}_{22}{}^T\hat{S}_{22}^{'}\tilde{V}_{22}{}^T\bar{Z}_{22} - d_{u22} - \hat{K}_{22}{}^T\bar{\varphi}_{22} + d_{a22}\end{bmatrix}\right\}.$$

Let the weight update laws be

$$\begin{aligned}\dot{\hat{W}}_{2j} &= \Gamma_{w2j}[(\hat{S}_{2j} - \hat{S}_{2j}^{'}\hat{V}_{2j}{}^T\bar{Z}_{2j})e_{2j} - \sigma_{w2j}\hat{W}_{2j}], \\ \dot{\hat{V}}_{2j} &= \Gamma_{v2j}[\bar{Z}_{2j}\hat{W}_{2j}{}^T\hat{S}_{2j}^{'}e_{2j} - \sigma_{v2j}\hat{V}_{2j}], \\ \dot{\hat{K}}_{2j} &= \Gamma_{k2j}[\bar{\phi}_{2j}e_{2j} - \sigma_{k2j}\hat{K}_{2j}],\end{aligned}$$

and using the facts (8), and

$$\begin{aligned}&2\tilde{W}^T\hat{W} = \left\|\tilde{W}\right\|^2 + \left\|\hat{W}\right\|^2 - \left\|W^*\right\|^2 \geq \left\|\tilde{W}\right\|^2 - \left\|W^*\right\|^2, \\ &2tr\left\{\tilde{V}^T\hat{V}\right\} = \left\|\tilde{V}\right\|_F^2 + \left\|\hat{V}\right\|_F^2 - \left\|V^*\right\|_F^2 \geq \left\|\tilde{V}\right\|_F^2 - \left\|V^*\right\|_F^2,\end{aligned}$$

the time derivative of the Lyapunov function

$$\begin{aligned}V_2 = V_1 &+ \frac{1}{2}e_2^T g_2^{-1} e_2 + \frac{1}{2}\sum_{j=1}^{2}\Big(\tilde{W}_{2j}^T\Gamma_{w2j}^{-1}\tilde{W}_{2j} \\ &+ tr\left\{\tilde{V}_{2j}^T\Gamma_{v2j}^{-1}\tilde{V}_{2j}\right\} + \tilde{K}_{2j}^T\Gamma_{k2j}^{-1}\tilde{K}_{2j}\Big),\end{aligned}$$

derived similar to that in step 1, is given by

$$\begin{aligned}\dot{V}_2 \leq\ & e_2^T e_3 - \sum_{j=1}^{2}\left(\sigma_{w2j}\left\|\tilde{W}_{2j}\right\|^2/2 + \sigma_{v2j}\left\|\tilde{V}_{2j}\right\|_F^2/2\right) \\ & - \sum_{i=1}^{2}\left(e_i^T c_i e_i - \xi_i\right) - \sum_{i=1}^{2}\sum_{j=1}^{2}\left(\sigma_{kij}\left\|\tilde{K}_{ij}\right\|^2/2\right),\end{aligned}$$

where

$$\xi_2 = \sum_{j=1}^{2}\Big[0.2785\mu_{2j}\left(\left\|V_{2j}^*\right\|_F + \left\|W_{2j}^*\right\| + \left\|W_{2j}^*\right\|_1 + \varepsilon_{2jU} + d_{a2jU}\right)$$
$$+\sigma_{w2j}\left\|W_{2j}^*\right\|^2/2 + \sigma_{v2j}\left\|V_{2j}^*\right\|_F^2/2 + \sigma_{k2j}\left\|K_{2j}^*\right\|^2/2\Big].$$

Step 3:

This step is similar to step 1. Let the virtual control law be

$$x_{4d} = -e_2 - c_3 e_3 + \dot{x}_{3d} + u_{4dvsc} = \left[x_{41d}, x_{42d}\right]^T.$$

We use the smooth variable structure control law as $u_{4dvsc} = \left[u_{4dvsc1}, u_{4dvsc2}\right]^T$, where

$$u_{4dvscj} = -\hat{K}_{3j}\bar{\phi}_{3j} = -\hat{K}_{3j}\left(\frac{2}{\pi}\arctan\left(\frac{e_{3j}}{\mu_{3j}}\right)\right).$$

The weight update law is $\dot{\hat{K}}_{3j} = \Gamma_{k3j}[\bar{\phi}_{3j}e_{3j} - \sigma_{k3j}\hat{K}_{3j}]$.

Using a similar derivation to that in step 1, the time derivative of the Lyapunov function

$$V_3 = V_1 + V_2 + \frac{1}{2}e_3^T e_3 + \frac{1}{2}\sum_{j=1}^{2}\tilde{K}_{3j}^T\Gamma_{k3j}^{-1}\tilde{K}_{3j},$$

is given by

$$\dot{V}_3 \le e_3^T e_4 - \sum_{j=1}^{2}\left(\sigma_{w2j}\left\|\tilde{W}_{2j}\right\|^2/2 + \sigma_{v2j}\left\|\tilde{V}_{2j}\right\|_F^2/2\right)$$
$$-\sum_{i=1}^{3}\left(e_i^T c_i e_i - \xi_i\right) - \sum_{i=1}^{3}\sum_{j=1}^{2}\left(\sigma_{kij}\left\|\tilde{K}_{ij}\right\|^2/2\right),$$

where $\xi_3 = \sum_{j=1}^{2}\left(0.2785\mu_{3j}d_{a3jU} + \sigma_{k3j}\left\|K_{3j}^*\right\|^2/2\right)$.

Step 4:

This is the last step and is similar to that in step 2. Let the actual control law be

$$u = -e_3 - c_4 e_4 - \begin{bmatrix}\hat{W}_{41}^T S_{41}(\hat{V}_{41}^T\bar{Z}_{41})\\ \hat{W}_{42}^T S_{42}(\hat{V}_{42}^T\bar{Z}_{42})\end{bmatrix} + u_{5dvsc} = \left[u_1, u_2\right]^T.$$

The smooth variable structure control law is $u_{5dvsc} = \left[u_{5dvsc1}, u_{5dvsc2}\right]^T$, where

$$u_{5dvscj} = -\hat{K}_{4j}{}^T\bar{\phi}_{4j},$$

$$\bar{\phi}_{4j} = \begin{bmatrix}\left\|\bar{Z}_{4j}\hat{W}_{4j}^T\hat{S}_{4j}^{'}\right\|_F\dfrac{2}{\pi}\arctan\left(\dfrac{e_{4j}}{\mu_{4j}}\left\|\bar{Z}_{4j}\hat{W}_{4j}^T\hat{S}_{4j}^{'}\right\|_F\right)\\ \left\|\hat{S}_{4j}^{'}\hat{V}_{4j}^T\bar{Z}_{4j}\right\|\dfrac{2}{\pi}\arctan\left(\dfrac{e_{4j}}{\mu_{4j}}\left\|\hat{S}_{4j}^{'}\hat{V}_{4j}^T\bar{Z}_{4j}\right\|\right)\\ \dfrac{2}{\pi}\arctan\left(\dfrac{e_{4j}}{\mu_{4j}}\right)\end{bmatrix}.$$

Let the weight update laws be

$$\dot{\hat{W}}_{4j} = \Gamma_{w4j}[(\hat{S}_{4j} - \hat{S}_{4j}^{'}\hat{V}_{4j}^{'T}\bar{Z}_{4j})e_{4j} - \sigma_{w4j}\hat{W}_{4j}],$$
$$\dot{\hat{V}}_{4j} = \Gamma_{v4j}[\bar{Z}_{4j}\hat{W}_{4j}{}^T\hat{S}_{4j}^{'}e_{4j} - \sigma_{v4j}\hat{V}_{4j}],$$
$$\dot{\hat{K}}_{4j} = \Gamma_{k4j}[\bar{\phi}_{4j}e_{4j} - \sigma_{k4j}\hat{K}_{4j}].$$

The time derivative of the Lyapunov function

$$V_4 = V_1 + V_2 + V_3 + \frac{1}{2}e_4^T g_4^{-1}e_4 + \frac{1}{2}\sum_{j=1}^{2}\Big(\tilde{W}_{4j}^T\Gamma_{w4j}^{-1}\tilde{W}_{4j}$$
$$+tr\left\{\tilde{V}_{4j}^T\Gamma_{v4j}^{-1}\tilde{V}_{4j}\right\} + \tilde{K}_{4j}^T\Gamma_{k4j}^{-1}\tilde{K}_{4j}\Big),$$

derived similar to that in step 2, is given by

$$\dot{V}_4 \le -\sum_{j=1}^{2}\left(\sigma_{w2j}\left\|\tilde{W}_{2j}\right\|^2/2 + \sigma_{v2j}\left\|\tilde{V}_{2j}\right\|_F^2/2\right)$$
$$-\sum_{j=1}^{2}\left(\sigma_{w4j}\left\|\tilde{W}_{4j}\right\|^2/2 + \sigma_{v4j}\left\|\tilde{V}_{4j}\right\|_F^2/2\right)$$
$$-\sum_{i=1}^{4}\left(e_i^T c_i e_i - \xi_i\right) - \sum_{i=1}^{4}\sum_{j=1}^{2}\left(\sigma_{kij}\left\|\tilde{K}_{ij}\right\|^2/2\right),$$

where

$$\xi_4 = \sum_{j=1}^{2}\Big[0.2785\mu_{4j}\left(\left\|V_{4j}^*\right\|_F + \left\|W_{4j}^*\right\| + \left\|W_{4j}^*\right\|_1 + \varepsilon_{4jU} + d_{a4jU}\right)$$
$$+\sigma_{w4j}\left\|W_{4j}^*\right\|^2/2 + \sigma_{v4j}\left\|V_{4j}^*\right\|_F^2/2 + \sigma_{k4j}\left\|K_{4j}^*\right\|^2/2\Big].$$

Let

$$\varsigma = \min\left\{\min_{i=1,3}\left\{\frac{c_i}{0.5}\right\}, \min_{j=2,4}\left\{\frac{c_j}{0.5\left\|g_j^{-1}\right\|}\right\}\right\} > 0,\ \delta = \sum_{k=1}^{4}\xi_k \ge 0$$

and choose

$$\sigma_{wlj} \ge \varsigma\lambda_{\max}\left\{\Gamma_{wlj}^{-1}\right\}, \sigma_{vlj} \ge \varsigma\lambda_{\max}\left\{\Gamma_{vlj}^{-1}\right\},$$
$$\sigma_{kij} \ge \varsigma\lambda_{\max}\left\{\Gamma_{kij}^{-1}\right\};\ l = 2,4;\ i = 1,\ldots,4;\ j = 1,2,$$

we have $\dot{V}_4 \le -\varsigma V_4 + \delta$.

From this point on, you can use a standard nonlinear analysis technique given, for example, in [14] to conclude that all error trajectories are globally uniformly ultimately bounded.

IV. Simulation Results

We use the robot model (1) with parameter values from an actual experiment to represent the actual robot in our simulation.

We simulate deadzone and backlash using the following parameters. For deadzone model (2), we have $d^- = -0.1, d^+ = 0.1, m^- = m^+ = 1$. For backlash model (3), we use $d^- = -0.1, d^+ = 0.1, m = 1$.

External disturbances are as follows:

$$d_{a1} = d_{a4} = [0.001\sin(\theta_1\dot{\theta}_1), \arctan(\theta_1\dot{\theta}_2)]^T,$$
$$d_{a2} = d_{a3} = [0.001\,\mathrm{randn}(2,1)]^T,$$

where *randn* represents white noise.

To simulate payload changes, we multiply $M(x_1)$ and $V(x_1, x_2)$ matrices by three during 10 to 20 s and 30 to 40 s.

There are 4 neural networks; each has 5 hidden nodes. Inputs to each neural network are

$$\bar{Z}_{21} = \{x_{11}, x_{12}, x_{21}, x_{22}, \dot{x}_{21d}, 1\},$$
$$\bar{Z}_{22} = \{x_{11}, x_{12}, x_{21}, x_{22}, \dot{x}_{22d}, 1\},$$
$$\bar{Z}_{41} = \{x_{11}, x_{12}, x_{31}, x_{32}, x_{41}, x_{42}, \dot{x}_{41d}, 1\},$$
$$\bar{Z}_{42} = \{x_{11}, x_{12}, x_{31}, x_{32}, x_{41}, x_{42}, \dot{x}_{42d}, 1\}.$$

Neural network and controller design parameters are as follows:

$$\Gamma_{wij} = \Gamma_{vij} = \Gamma_{kij} = 10, c_i = 10,$$
$$\sigma_{wij} = \sigma_{vij} = \sigma_{kij} = 0.2, \mu = 0.1.$$

Input saturation limits are set at ± 15. All initial values are

set to zeros. Sampling period is 1 ms. The desired trajectory is obtained from passing a square wave signal of amplitude 10, with zero mean, and 20-second period into the filter $1/(s+2)^3$.

Fig. 4 contains scatter plots that show deadzone and backlash. In Fig. 5, the control system achieves good overall tracking performance as can be seen from the results in parts (a) to (d). Parts (e) and (f) show control inputs that actually drive the plant. Parts (g) and (h) show the actual functions h_{21} and h_{22} versus their estimated values $\hat{h}_{21}$ and $\hat{h}_{22}$. Parts (i) and (j) verify Assumption 3 by plotting $e_2^T g_2^{-1} e_2$ and $e_4^T g_4^{-1} e_4$.

V. Conclusion

The controller achieves good tracking performance. However, there are some interesting issues left as future work. First, we assume that the actual plant is in a nonlinear form (1). The actual robot may not belong exactly to this form, which may degrade the controller performance. Second, we need to have an effective way to measure the significance of the dropped terms in the kinetic energy.

References

[1] L. M. Sweet and M. C. Good, "Re-definition of the robot motion control problem: effects of plant dynamics drive system constraints, and user requirements," *Proc. of 23rd IEEE Conf. on Decision and Control*, Las Vegas, NV, 1984, pp. 724-731.

[2] M. W. Spong, "Modeling and control of elastic joint robots," *Trans. ASME J. Dynamic Systems, Measurement and Control*, vol. 109, no. 4, pp. 310-319, 1987.

[3] S. S. Ge, "Adaptive control design for flexible joint manipulators," *Automatica*, vol. 32, no. 2, pp. 273-278, 1996.

[4] M. Spong and M. Vidyasagar, *Robot Dynamics and Control*. New York: Wiley, 1989.

[5] A, De Luca and P. Lucibello, "A general algorithm for dynamic feedback linearization of robots with elastic joints," *Proc. of 1998 IEEE Int. Conf. on Robotics and Automation*, Belgium, pp. 504-510.

[6] B. Brogliato, R. Ortega, and R. Lozano, "Global tracking controllers for flexible-joint manipulators: a comparative study," *Automatica*, vol. 31, no. 7, pp. 941-956, 1995.

[7] S. S. Ge, T. H. Lee, and C. J. Harris, *Adaptive Neural Network Control of Robotic Manipulators*. Singapore: World Scientific Publishing, 1998, ch. 7.

[8] A. C. Huang and Y. C. Chen, "Adaptive sliding control for single-link flexible-joint robot with mismatched uncertainties," *IEEE Trans. Contr. Syst. Technol.,* vol. 12, no. 5, pp. 770-775, 2004.

[9] C. W. Park, "Robust stable fuzzy control via fuzzy modeling and feedback linearization with its applications to controlling uncertain single-link flexible joint manipulators," *Journal of Intelligent and Robotic Systems*, vol. 39, pp. 131-147, 2004.

[10] G. Tao and P. V. Kokotovic, *Adaptive Control of Systems with Actuator and Sensor Nonlinearities*. New York: Wiley, 1996.

[11] F. L. Lewis, J. Campos, and R. Selmic, *Neuro-Fuzzy Control of Industrial Systems with Actuator Nonlinearities*. Philadelphia: SIAM, 2002.

[12] K. I. Funahashi, "On the approximate realization of continuous mappings by neural networks," *Neural Networks*, vol. 2, pp. 183-192, 1989.

[13] S. S. Ge, C. C. Hang, T. H. Lee, and T. Zhang, *Stable Adaptive Neural Network Control*. The Netherlands: Kluwer, 2002.

[14] J. T. Spooner, M. Maggiore, R. Ordonez and K. M. Passino, *Stable Adaptive Control and Estimation for Nonlinear Systems*. New York: Wiley Interscience, 2002, ch. 2.

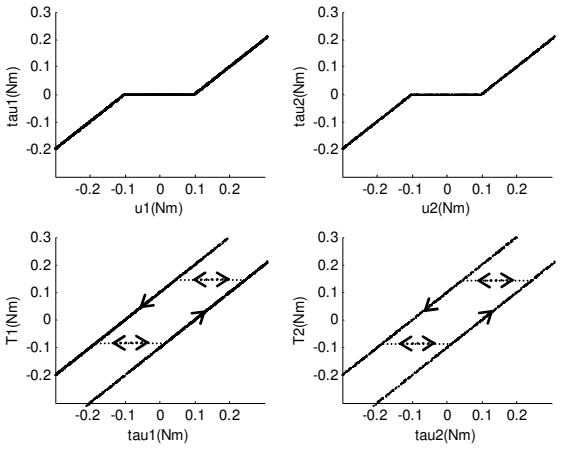

Fig. 4. Scatter plots showing deadzone and backlash. (Top-left) Plot between u_1 and τ_1. (Top-right) Plot between u_2 and τ_2. (Bottom-left) Plot between τ_1 and T_1. (Bottom-right) Plot between τ_2 and T_2.

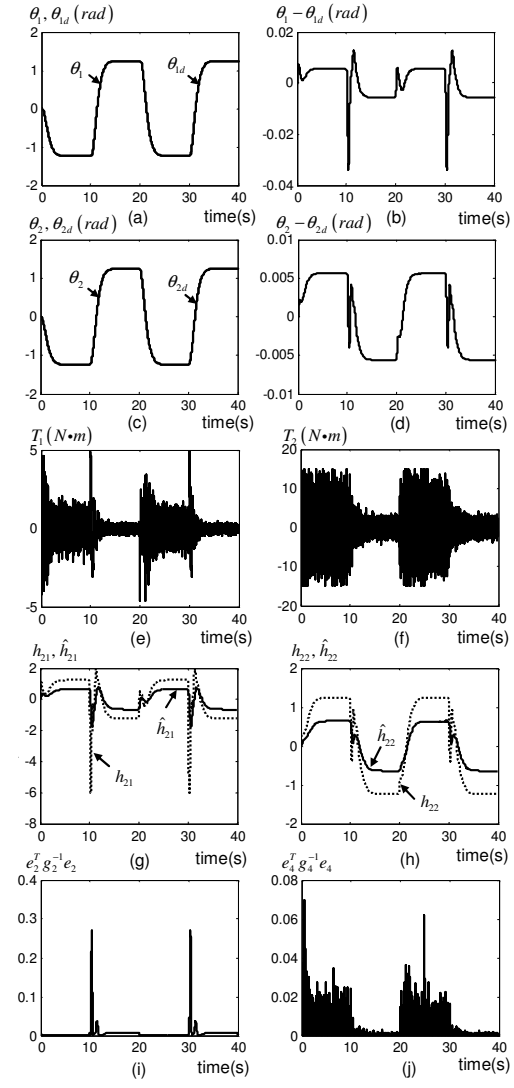

Fig. 5. Simulation results in 40 seconds. (a) θ_1 versus its desired trajectory θ_{1d}. (b) Tracking error $\theta_1 - \theta_{1d}$. (c) θ_2 versus its desired trajectory θ_{2d}. (d) Tracking error $\theta_2 - \theta_{2d}$. (e) Control input T_1. (f) Control input T_2. (g) Actual function h_{21} versus estimated function $\hat{h}_{21}$. (h) Actual function h_{22} versus estimated function $\hat{h}_{22}$. (i) To verify positive definiteness, $e_2^T g_2^{-1} e_2$. (j) To verify positive definiteness, $e_4^T g_4^{-1} e_4$.